

Taniborbactam Inhibits Cefepime-Hydrolyzing Variants of *Pseudomonas*-derived Cephalosporinase (PDC)

INTRODUCTION

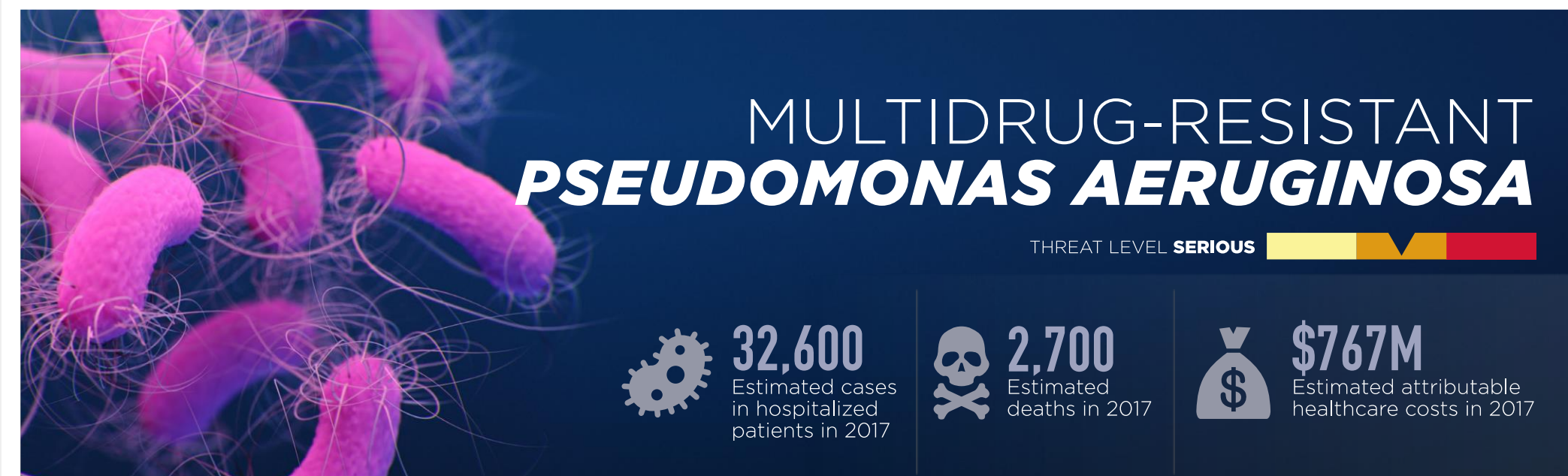


Figure 1: CDC Threat Assessment for Multidrug-resistant *Pseudomonas aeruginosa*. (1)

Pseudomonas aeruginosa, β -Lactamases, and Amino Acid Deletions

- P. aeruginosa* is a gram-negative pathogen responsible for many serious infections. Multidrug resistance in *P. aeruginosa* is classified as a "serious threat" by the CDC. (1)
- Pseudomonas*-derived cephalosporinase (PDC) is the major class C β -lactamase produced by *P. aeruginosa* and is a major cause of antibiotic resistance.
- PDC-88 is a variant characterized by a Thr-Pro amino acid deletion in the R2-loop (Δ 289-290; Fig. 1) (2)
- PDC-88 and other PDC R2-loop deletions reduce susceptibility to cefepime (FEP), ceftazidime (CAZ), and ceftolozane-tazobactam (C/T) (2), but the mechanism remains unstudied in PDC.

Cefepime and Taniborbactam

- Taniborbactam (TAN) is a novel cyclic boronate β -lactamase inhibitor (BLI) with activity against all four Ambler classes of β -lactamases (3).
- Cefepime (FEP) is a commonly used anti-*Pseudomonas* cephalosporin antibiotic.
- The β -lactam-BLI (BL-BLI) combination cefepime-taniborbactam (FTB; Fig 2) is currently in phase 3 clinical trials.

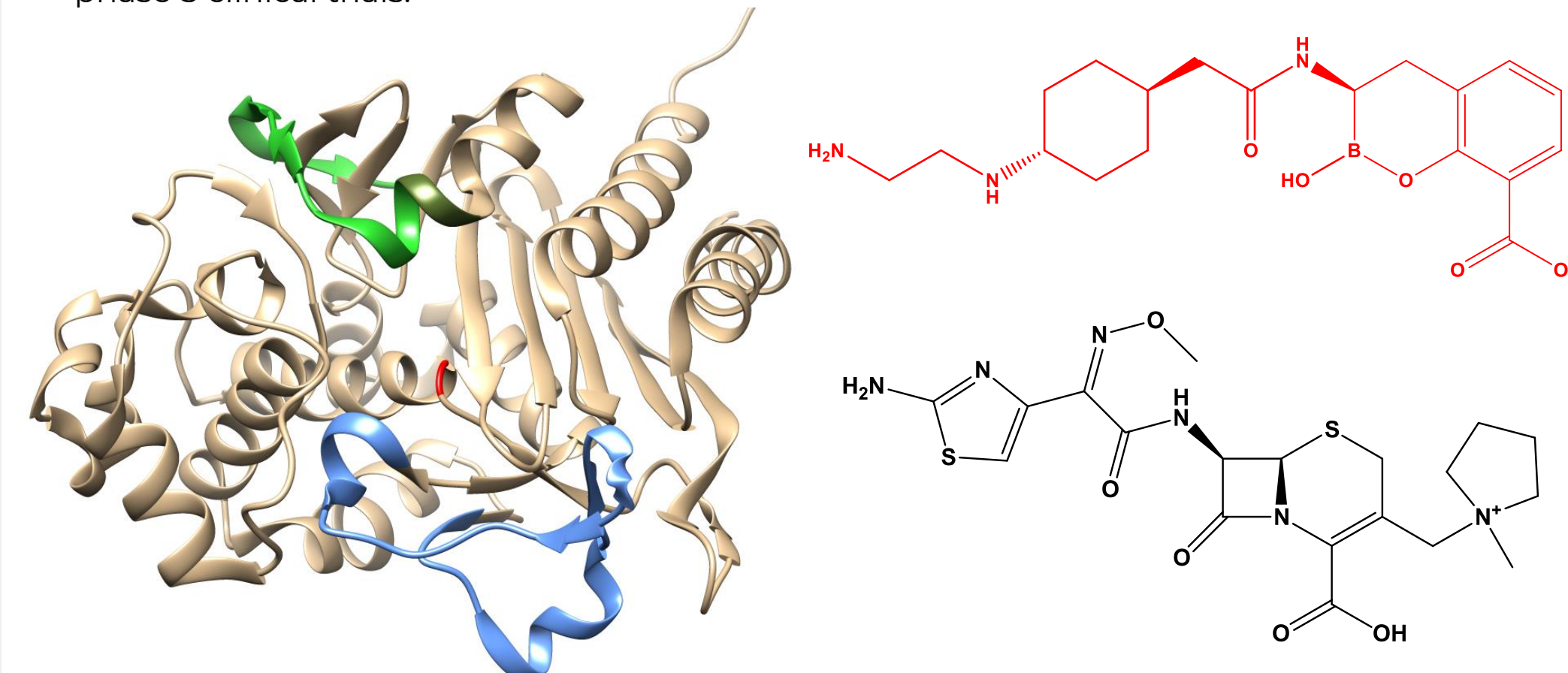


Figure 2: Crystal structure of PDC. The R2-loop (our region of interest) is in green and the deleted residues in olive. The Ω -loop (blue) and catalytic Serine 64 (red) are included for reference. PDB ID: 4GZB

Figure 3: Structures of cefepime (β -lactam antibiotic; black, bottom) and taniborbactam (novel β -lactamase inhibitor; red, top).

Materials and Methods

Minimum Inhibitory Concentrations (MICs)

- Broth microdilution MICs were determined in accordance with CLSI M07 guidelines. Isogenic *E. coli* strains expressing plasmid-encoded PDC variants were used.

Enzyme Kinetic Characterization

- Kinetics were determined spectrophotometrically by tracking substrate hydrolysis (ATM, CAZ, FEP, TOL) or inhibition of nitrocefin (a reporter substrate) hydrolysis (AVI, TAN, TAZO).

Mass Spectrometry

- Timed incubations were conducted with enzyme and 2- to 100-fold excess of substrate. Data was collected using a Waters Synapt G2-Si Quadrupole time-of-flight (Q-TOF) instrument.

Circular Dichroism

- Thermal stability was assessed by tracking the proportion of enzyme folded at several UV wavelength across the range of 20°C to 70°C to determine the melting point (T_m).

Molecular Modeling and Docking

- Molecular modeling was performed using BIOVIA Discovery Studio 2017 with the included modeling, docking, and analysis modules.

RESULTS

PDC R2-Loop Deletions Elevate FEP & TOL MICs

Species	Strain	Sequence Changes	FEP				TOL	
			Alone	TAN	AVI	TAZO	Alone	TAZO
<i>E. coli</i>	DH10B/pTU501 (vector)	N/A	0.25	0.12	0.12	0.12	1	0.5
<i>E. coli</i>	DH10B/pTU606 (PDC-1)	Comparator	1	0.25	0.25	1	4	4
<i>E. coli</i>	DH10B/pTU609 (PDC-3)	T79A	2	0.25	0.12	1	8	4
<i>E. coli</i>	DH10B/pTU625 (PDC-88)	G1D, T79A, V178L Δ 289-290, V329I, G364A	32	0.25	0.25	8	>32	16
<i>E. coli</i>	DH10B/pTU626 (PDC-89)	G1D, T79A, V178L Δ 289-291, G364A	32	0.25	0.25	16	16	16
<i>E. coli</i>	DH10B/pTU627 (PDC-90)	G1D, T79A, V178L Δ 289-291, V329I, G364A	32	0.25	0.5	32	32	16
<i>E. coli</i>	DH10B/pTU628 (PDC-91)	G1D, T79A, V178L Δ 289-291, V329I, G364A	32	0.5	0.25	32	32	16
<i>E. coli</i>	DH10B/pTU629 (PDC-92)	G1D, T79A, V178L Δ 293-294, G364A	32	0.25	0.25	32	16	8

Table 1: Minimum inhibitory concentrations (MICs) for isogenic *E. coli* expressing PDC β -lactamase constructs. Values in mcg/mL. FEP, cefepime; TOL, ceftolozane; TAN, taniborbactam; AVI, avibactam; TAZO, tazobactam. Inhibitors were used at a constant 4 mcg/mL.

PDC-88 Increases Efficiency of FEP Hydrolysis

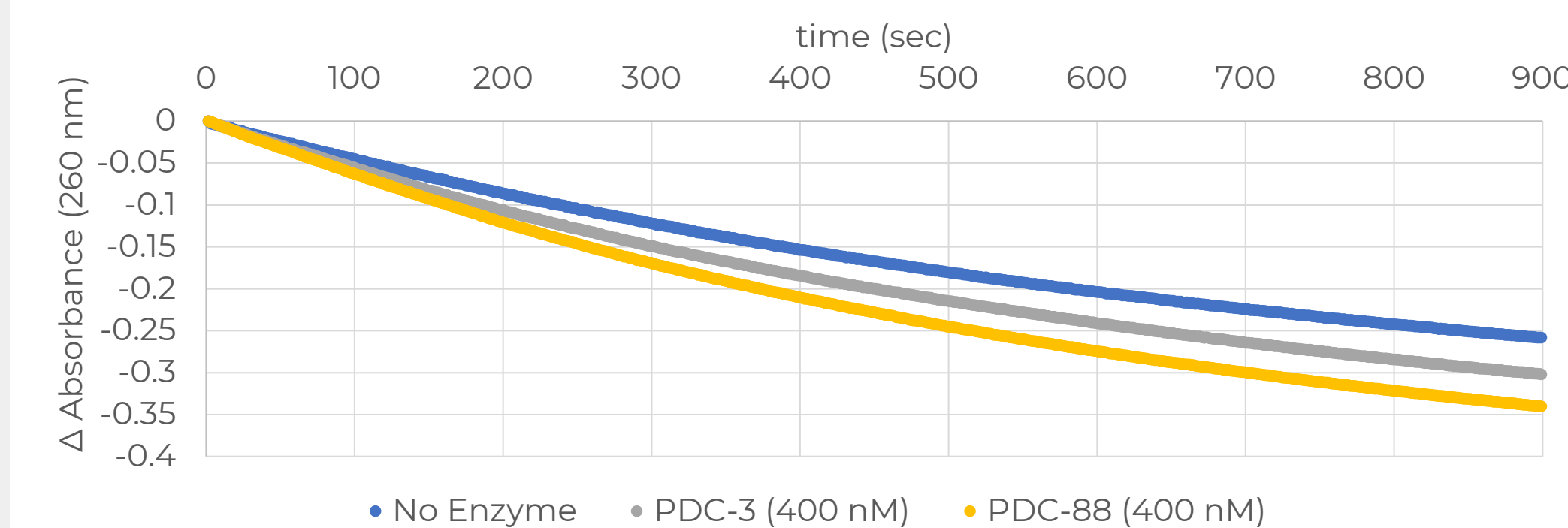


Figure 4: Spectrophotometric progress curves of FRP hydrolysis collected at 260 nm. PDC-88 hydrolyzes FEP more efficiently than PDC-3. A no enzyme control is included to account for background hydrolysis.

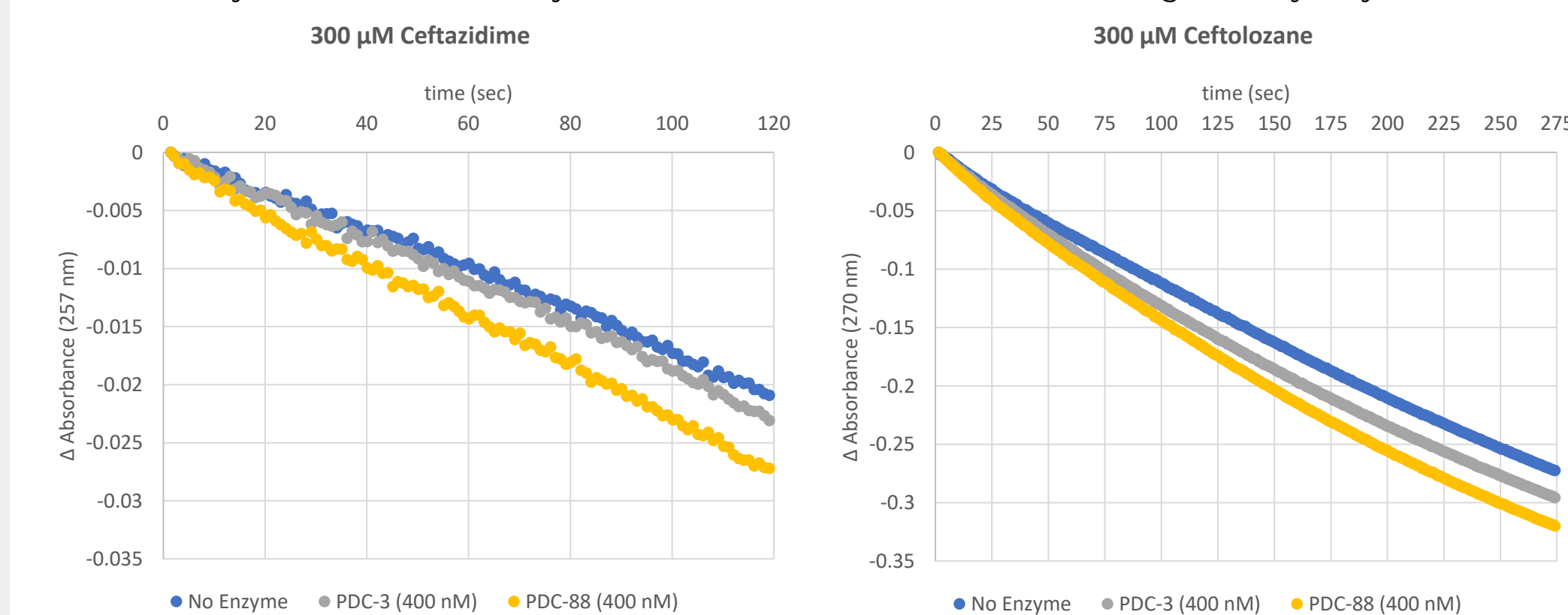


Figure 5: Spectrophotometric progress curves for CAZ and TOL collected at 257 nm and 270 nm respectively. In comparison to FEP, the R2-loop deletion has much less impact on CAZ and TOL hydrolysis.

CONCLUSIONS

- Different kinetic constants are responsible for the elevated cephalosporin MICs. We posit that PDC-88 increases FEP MIC by enhanced hydrolysis; TOL MICs by enabling acylation; and CAZ MICs by covalent trapping.
- TAN inhibits both PDC-3 and PDC-88 with similar kinetic profiles. Notably, TAN appears to be a more efficient inhibitor of PDC (lower K_m , higher k_2/K_m values) than current BLIs targeted for use against *P. aeruginosa*.
- The combination of TAN and FEP may represent an important treatment option for *P. aeruginosa* isolates that develop extended-spectrum AmpC (ESAC) phenotypes.

Kinetics Provide Insight into Hydrolytic Changes

Substrate	PDC-3			PDC-88		
	k_{cat} (s^{-1})	K_m (μM)	k_{cat}/K_m ($\mu M^{-1}s^{-1}$)	k_{cat} (s^{-1})	K_m (μM)	k_{cat}/K_m ($\mu M^{-1}s^{-1}$)
Cefepime	0.51 ± 0.04	227 ± 9	0.0020 ± 0.0002	0.15 ± 0.01	26 ± 2	0.0060 ± 0.0006

Table 2: A roughly three-fold decrease in turnover (k_{cat}) is countered by a nearly-ten-fold decrease in the Michaelis constant (K_m) to produce an overall three-fold increase in catalytic efficiency (k_{cat}/K_m) for PDC-88 compared to PDC-3. This suggests improved FEP binding plays an important role in the hydrolytic changes.

AVI and TAN Both Effectively Inhibit PDC-3 and PDC-88

Enzyme	Inhibitor	K_i app (μM)	k_2/K_m ($M^{-1}s^{-1}$)	IC_{50} (μM)	k_{cat}/k_{inact}	k_{off} (s^{-1})	$t_{1/2}$ (s)
PDC-3	AVI	2.7 ± 0.3	$24,200 \pm 2,400$	0.049 ± 0.005	1	0.00180 ± 0.00010	385
	TAN	0.66 ± 0.07	$160,000 \pm 23,000$	0.016 ± 0.002	2	0.0012 ± 0.0001	577
	TAZO	27 ± 3	$1,200 \pm 120$	0.9 ± 0.1	50	ND	ND
PDC-88	AVI	5.5 ± 0.6	$12,000 \pm 1,200$	0.061 ± 0.007	1	0.00010 ± 0.00005	6931
	TAN	0.61 ± 0.06	$142,600 \pm 14,000$	0.022 ± 0.002	2	0.0007 ± 0.0001	990
	TAZO	58 ± 6	400 ± 40	2.2 ± 0.3	30	ND	ND

Table 3: Kinetic characterization of the ability of AVI, TAN, and TAZO to inhibit PDC. As expected, TAZO is a kinetically poor inhibitor of PDC. TAN has a lower inhibition constant (K_i) and higher acylation rate (k_2/K_m) suggesting it more easily forms an acyl-enzyme complex with PDC, but AVI has a lower deacylation rate (k_{off}) and longer half-life ($t_{1/2}$) suggesting the complex is more stable. Together, these help to explain why AVI and TAN are microbiologically indistinguishable with strains expressing PDC.

PDC-88 has Similar Stability to PDC-3 & TAN stabilizes both more than TAZO

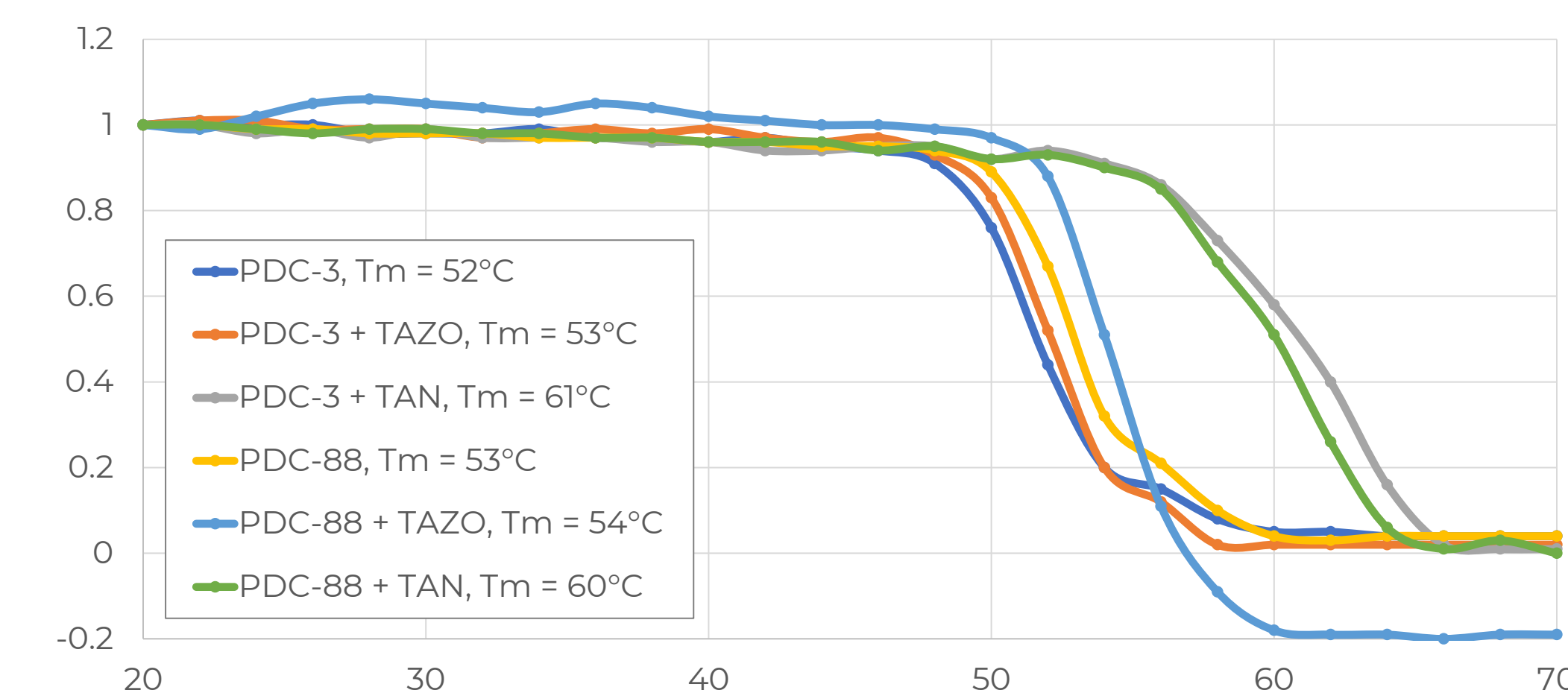


Figure 3: Circular dichroism thermal denaturation curves for PDC-3 and PDC-88 with and without TAN and TAZO. Stability is nearly unchanged between PDC-3 and PDC-88. TAZO only increased the melting points (T_m) by 1°C whereas TAN provides a 9°C for increase PDC-3 and 7°C for PDC-88, as anticipated from a very good inhibitor.

REFERENCES

- Centers for Disease Control and Prevention. (2019). Antibiotic Resistance Threats in the United States, 2019.
- Berrazeg, M. Jeannot, K. Ntsogo Enguéné, VY. Broutin, I. Loeffert, S. Fournier, D. Plésiat, P. (2015). Mutations in β -Lactamase AmpC Increase Resistance of *Pseudomonas aeruginosa* Isolates to Antipseudomonal Cephalosporins. *Antimicrobial Agents and Chemotherapy*, 59(10), 6248-55.
- Hamrick JC, Docquier JD, Uehara T, Myers CL, Six DA, Chatwin CL, John KJ, Vernacchio SF, Cusick SM, Trout REL, Pozzi C, De Luca F, Benvenuti M, Mangani S, Liu B, Jackson RW, Moock G, Xerri L, Burns CJ, Pevear DC, Daigle DM. VNRX-5133 (Taniborbactam), a Broad-Spectrum Inhibitor of Serine- and Metallo- β -Lactamases, Restores Activity of Cefepime in *Enterobacteriales* and *Pseudomonas aeruginosa*. *Antimicrob Agents Chemother*. 2020 Feb 21;64(3):e01963-19.

Mass Spectrometry Reveals Mechanistic Detail

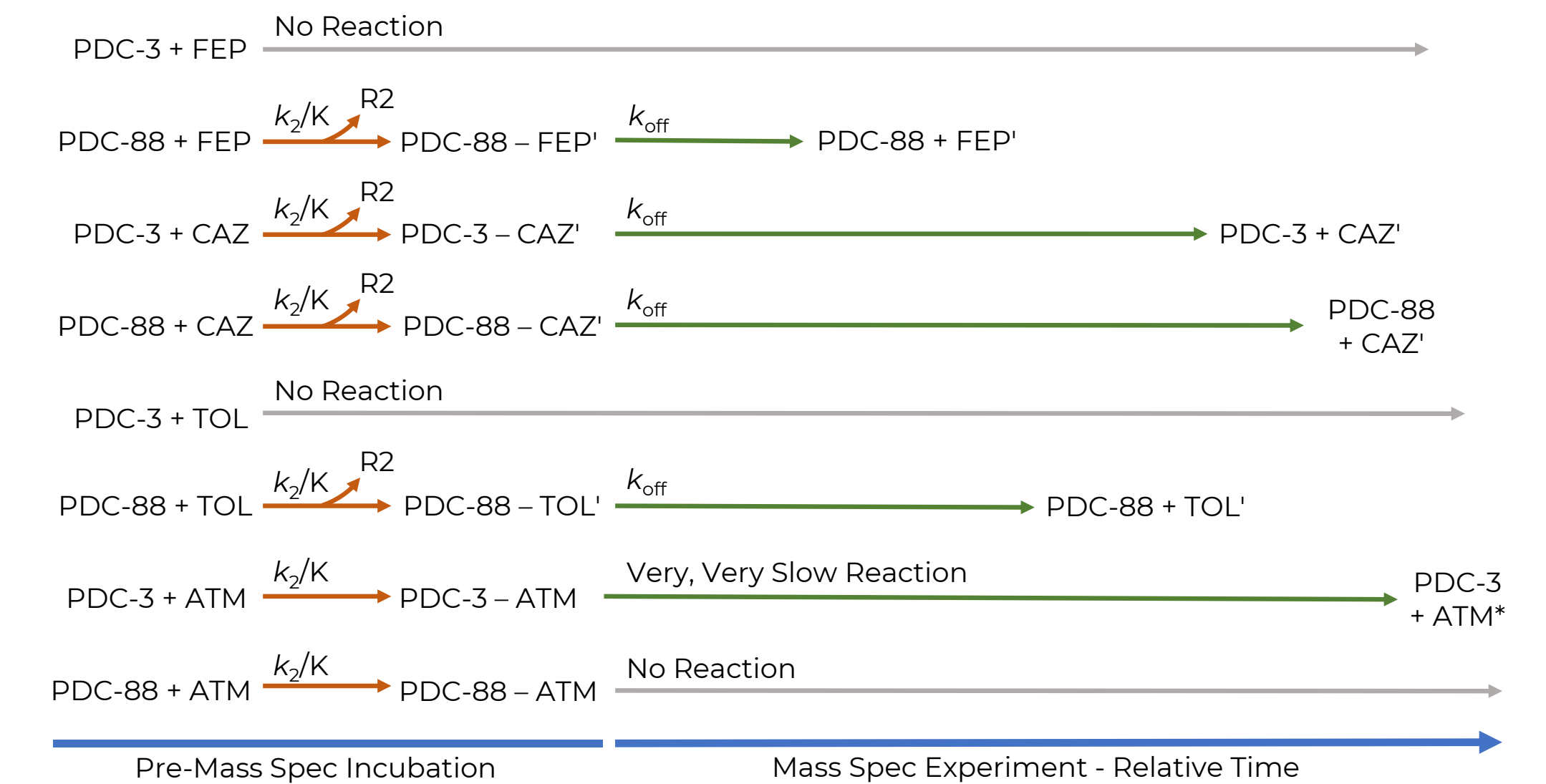


Figure 5: Graphical summary of mass spectrometry results. FEP does not react with PDC-3 but is acylated and quickly (relative to other substrates) hydrolyzed by PDC-88. CAZ is acylated and hydrolyzed by both variants but appears to be hydrolyzed slightly slower in PDC-88. TOL does not react with PDC-3 but is acylated by PDC-88 and is hydrolyzed (very, very slowly) by PDC-3 but not at all by PDC-88 (within 60 minutes of monitoring).

Molecular Modeling Suggests Structural Changes

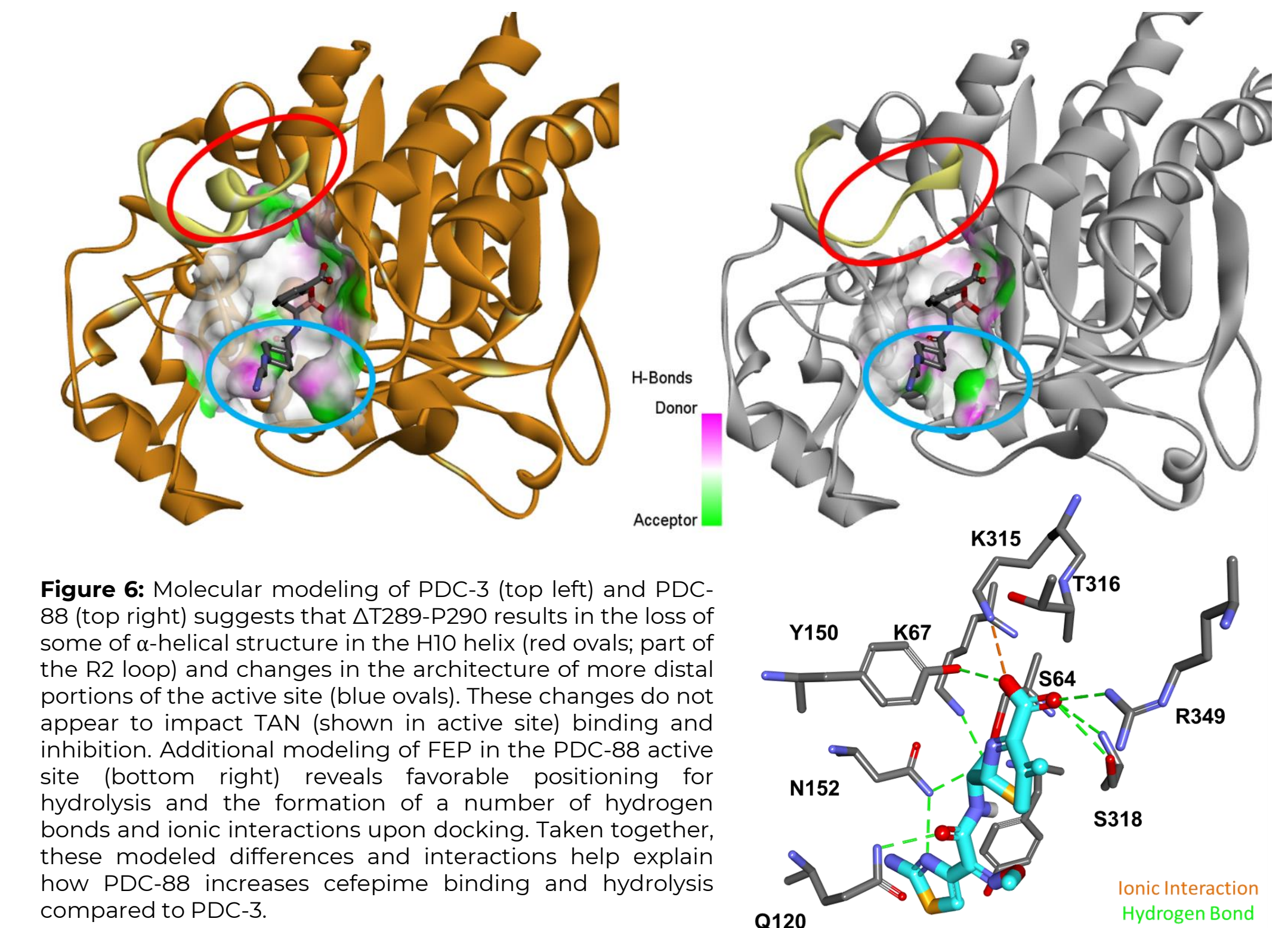


Figure 6: Molecular modeling of PDC-3 (top left) and PDC-88 (top right) suggests that Δ T289-P290 results in the loss of some of α -helical structure in the H10 helix (red ovals; part of the R2 loop) and changes in the architecture of more distal portions of the active site (blue ovals). These changes do not appear to impact TAN (shown in active site) binding and inhibition. Additional modeling of FEP in the PDC-88 active site (bottom right) reveals favorable positioning for hydrolysis and the formation of a number of hydrogen bonds and ionic interactions upon docking. Taken together, these modeled differences and interactions help explain how PDC-88 increases cefepime binding and hydrolysis compared to PDC-3.

ACKNOWLEDGEMENTS

Research reported herein was funded by Venatorx Pharmaceuticals, Inc. as a Cooperative Research and Development Agreement with R.A.B. and K.M.P.-W. Additional funds and/or facilities provided by the Cleveland Department of Veterans Affairs to R.A.B. and K.M.P.-W., the Veterans Affairs Merit Review Program Awards 1101BX001974 (R.A.B.) and 1101BX002872 (K.M.P.-W.) from the Biomedical Laboratory Research & Development Service of the VA Office of Research and Development, the Geriatric Research Education and Clinical Center VISN 10 (R.A.B.) and the National Institute of Allergy and Infectious Diseases of the National Institutes of Health under Award Numbers R21AI114508, R01AI100560, R01AI063517, and R01AI072219 to R.A.B. The content is solely the responsibility of the authors and does not necessarily represent the official views of the National Institutes of Health or the Department of Veterans Affairs.